Method of Automatic Artifacts Selection in Encephalography [1]

Riad Taha. Al-Kasasbeh[2] **B. Lvov[3]**

Abstract

An attempt is made to develop a method for automatic artifact selection in an electroencephalogram. Wavelet transform and artificial neural networks are combined with the analysis of statistical properties, based on the fractional dimension dynamics. Application of the method to experimental EEG signals showed that it can increase the reliability of artifacts selection.

Keywords: Electroencephalography, artifacts, wavelet, neural networks, fractals

[1] For the paper in Arabic see pages (39-40).

[2] Al-Balqa' Applied University- Amman.
[3] Al-Balqa' Applied University- Amman.

1. Introduction

In human brain activity analysis of electroencephalography (EEG) is one of the most important techniques. EEG signal is the electric potential on the surface of scalp caused by the physiological activities of the brain. Despite the development of modern techniques such as CT, MRI and others, electroencephalography still remains one of the best for nondestructive testing of brain functioning. But being a noninvasive tool encephalography meets strong difficulties caused by various mechanical and electrical interferences. Normal amplitude of EEG signals at scalp electrodes does not exceed several microvolts while other electrical potentials on the body surface like electrocardiogram can easily reach the level of mille-volts. Therefore, EEG analysis requires sophisticated signal processing. Widely known spectral decomposition of EEG signals [1-3] into rhythms occupying different frequencies bands, from 0.5 Hz to more than 40 Hz, is enriched by new methods of quantitative analysis. Among them are wavelet transform, neural network methods, modeling, entropy and fractal methods [4-6]. These special methods were used in attempts to overcome difficulties caused by non-stationary character of the clinical EEG signals.

Multiple problems in EEG signal processing come from various non-brain signals (artifacts) because of various mechanical and electrical interferences [7-10]. Traditionally, artifact detection is made by visual inspection of the encephalogram even if an automatic classification of transient time-varying EEG signal is used [11]. Visual inspection is reliable only if the artifact amplitude exceeds the regular activity signal. That is true for the most of automatic detection methods as well. But even if the artifact amplitude is small, statistical prosperities of the resulting signal can be changed drastically.

Recently, we can see a growing flow of publications with regard to the analysis of signal entropy, fractal structure or to the signal decomposition into deterministic and random components [12-14]. Calculation of fractal dimension can help to classify artifacts with different statistical properties, but models like fractal Brownian motion are developed for time-invariant processes [15-18]. In the present paper we present an attempt of plotting the dynamic fractal dimension and its subsequent analysis using wavelet transform and artificial neural network classifier.

The combination of these techniques helps to increase the reliability of artifact selection from EEG signals.

2. Fractal dimension dynamics.

The most important difference between regular EEG signal and artifact is in their statistical properties. Typical duration of a short artifact is from 0.1 to 1s. Within this time artifact signals should show higher level of correlation than a normal EEG signal.

Statistical properties of a signal can be estimated using different tools [17, 20] like correlation analysis, Kullback algorithm, fractal dimension definition etc. One of the ways is to present the signal as a fractal Brownian movement [16]. We choose a part of the signal (window) with the length L and make a linear regression presenting the signal inside the window as a straight line using the least square approximation. Next we estimate fluctuations of the signal from that straight line. Then we increase the length of the window and repeat the procedure. Plotting root mean square fluctuation Y as a function of the window length X in logarithmic scale should give us a straight line

$Y = B + Hx$ ……..(1)

For uncorrelated sequence H=1/2. And deviation of H from 1/2 shows the level of the sequence correlation. It can be explained with the aid of the model of fractal Brownian movement developed in the works of Mandelbrot, Van Ness and others [14-17].

Fractal Brownian movement with parameter H is a continuous function of time X(t) while

$\Delta X = X(t_2) - X(t_1)$……..……..(2)

where $t_2 > t_1$ is a random Gaussian sequence , that is

$$P(\Delta X < x) = \frac{1}{\sqrt{2\pi}\sigma(t_2 - t_1)^H} \int_{-\infty}^{x} \exp(-\tfrac{1}{2}(\frac{u}{\sigma(t_2 - t_1)^H})^2)du \text{ ….. (3)}$$

Fractal Brownian movement with H=1/2 coincides with the classical Brownian movement [16,17].

Variance of the fractal Brownian movement is

$$E[(X(t_2) - X(t_1))^2] = \sigma^2 |t_2 - t_1|^{2H} \text{ …… (4)}$$

As the variance depends only on the difference t_2 - t_1, then the increments Δ X do not depend on the time of observation. At H=1/2 dispersion is equal zero, and increments are independent (Markov process). If H≠1/2 then the increments are correlated, but still they are scale invariant, that is

$$\frac{1}{\sqrt{2\pi}\sigma r^H (t_2 - t_1)^H} \int_{-\infty}^{xr^H} \exp(-\tfrac{1}{2}(\frac{u}{\sigma r^H (t_2 - t_1)^H})^2) du = \quad \ldots.(5)$$

$$= \frac{1}{\sqrt{2\pi}\sigma (t_2 - t_1)^H} \int_{-\infty}^{x} \exp(-\tfrac{1}{2}(\frac{s}{\sigma (t_2 - t_1)^H})^2) ds, \quad s = u / r^H$$

And the distributions

$$X(t + \Delta t) - X(t) \quad \text{and} \quad \frac{1}{r^H}(X(t + r\Delta t) - X(t)$$

have the same mean value and variance, that is they are statistically equivalent.

Simple expression

$$d = 2 - H \quad \ldots\ldots (6)$$

shows the connection between the parameter H and the fractal dimension d [16].

In reality experimental EEG records can be considered as approximately scale invariant processes only over a short period of time close to 100…1000 ms. We cut the experimental EEG record into sections 2.5 seconds long each and applied the above described procedure to every section increasing window length from the minimum length 10ms to the maximum length 1s. The initial point of the window was put at the initial point of the chosen 2.5s section. The parameter H was calculated and then the window initial point to, was 10 ms shifted and the procedure was repeated and so long until the end of the longest 1s window touched the end of the 2.5s section. The result was a plot of H parameter or the fractal dimension of a signal (d =2-H) as a function of the window initial point To.

Several examples of a regular EEG signal taken from an encephalogram of a healthy volunteer sitting with open eyes in a shielded room are presented in the following figures. The experimental encephalogram was taken from an international 10-20 system of electrodes (see Fig.1 A, B, C)

The internationally standardized *10-20 system* is usually employed to record the spontaneous EEG. In this system 21 electrodes are located on the surface of the scalp, as shown in Figure 1A and Figure 1B. The positions are determined as follows: Reference points are *nasion*, which is the delve at the top of the nose, level with the eyes; and *inion*, which is the bony lump at the base of the skull on the midline at the back of the head. From these points, the skull perimeters are measured in the transverse and median planes. Electrode locations are determined by dividing these perimeters into 10% and 20% intervals. Three other electrodes are placed on each side equidistant from the neighboring points, as shown in Figure 1B [25].

In addition to the 21 electrodes of the international 10-20 system, intermediate 10% electrode positions are also used. The locations and nomenclature of these electrodes are standardized by the American Electroencephalographic Society[26] see Figure 1C). In this recommendation, four electrodes have different names compared to the 10-20 system; these are T_7, T_8, P_7, and P_8. These electrodes are drawn black with white text in the figure.

Besides the international 10-20 system, many other electrode systems exist for recording electric potentials on the scalp. The *Queen Square system* of electrode placement has been proposed as a standard in recording the pattern of evoked potentials in clinical testings [27].

The example shown in Fig.2a is a section of a regular EEG signal from a frontal F4 electrode. Fig. 2b shows H parameter of the same signal as a function of To. For comparison Fig.3a and Fig.3b present similar functions for an artifact caused by eyes movement and taken from the same F4 electrode. Eyes movement gives a strong signal at frontal electrodes (see Fig. 3a), and visual detection of such an artifact is not difficult. But *at the same time* the signal from the right temporal electrode T4 (see Fig.4a), shows a very slight difference from a regular activity signal (Fig.2a) and visual inspection can fail to detect such an artifact. The processing of the signal results in the function H (To) (see Fig.4b), which differs drastically from the similar function for the case of a regular activity (Fig.2b). Fig.5 presents a strong artifact signal from T4 electrode caused by a muscle movement . In figures 6 and 7 represented two kinds of original signal, detected with electrode configuration showed in figure 1. As we can see original EEG signal can be represented

in different amplitudes. At the same time the same muscle movement gives a weak artifact signal at the right parietal electrode P4 (see Fig.6). Signals shown at the next two figures are not proper artifact signals. They present regular EEG signals taken at the time when the patient was sitting with his eyes closed. Fig.7 shows the signal from P4 electrode (strong signal), while the signal shown at Fig.8 is taken from T4 electrode.

For automatic artifact selection a further signal processing was necessary. It included feature extraction and a classifier design.

3. Feature extraction

For feature extraction Multiresolution Wavelet Analysis (MRWA) was chosen. MRWA reflects the energy concentration in low and high frequency components. In addition, MRWA overcomes the fixed resolution problem and has been widely used in signal analysis, image denoising and compression [19-21].

The wavelet transform is a transformation to basis functions that are localized in scale and in time as well (where the Fourier transform is only localized in frequency, never giving any information about where in space or time the frequency happens). The frequency (similar in that sense to Fourier-related transforms) is derived from the scale. As basis functions one uses wavelets. These functions are scaled and convolved with the function you are analyzing all over the time axis.

The discrete wavelet transforms (DWT) of a signal x[n] is calculated by passing it through a series of filters. First the samples are passed through a low pass filter with impulse response g[n] resulting in a convolution of the two:

$$y[n] = x[n] * g[n] = \sum_{k=-\infty}^{\infty} x[k] \cdot g[n-k] \quad \text{.....(7)}$$

The signal is also decomposed simultaneously using a high-pass filter h[n]. The outputs giving the detail coefficients (from the high-pass filter), and approximation coefficients (from the low-pass). It is important that the two filters are related to each other and they are known as a quadrature mirror filter. However, since half the frequencies of the signal have now been removed, half the samples can be discarding according to Nyquist's rule. The filter outputs are then down-sampled (or sub-sampled) by 2:

$$y[n] = \sum_{k=-\infty}^{\infty} x[k] \cdot g[2n-k] \quad \text{..... (8)}$$

$$y_{high}[n] = \sum_{k=-\infty}^{\infty} x[k] \cdot h[2n-k] \quad \text{..... (9)}$$

This decomposition has halved the time resolution since only half of each filter output characterizes the signal (Fig 10.). However, each output has half the frequency band of the input so the frequency resolution has been doubled. This is in keeping with the Heisenberg Uncertainty Principle.

This decomposition is repeated to further increase the frequency resolution and

the approximation coefficients decomposed with high and low pass filters and

then down-sampled. This is represented as a binary tree with nodes representing

a sub-space with a different time-frequency localisation. The tree is known as a filter bank (fig 11).

At each level in the above diagram the signal is decomposed into low and high

frequencies. Due to the decomposition process the input signal must be a multiple of 2^n where n is the number of levels.

For example a signal with 16 samples, frequency range 0 to f_n and 3 levels of

decomposition, 4 output scales are produced:

Table 1. Example of wavelet transform

Level	**Frequencies**	**Samples**
3	**0 to f_n / 8**	**4**
	f_n / 8 to f_n / 4	**4**
2	**f_n / 4 to f_n / 2**	**8**
1	**f_n / 2 to f_n**	**16**

Frequency domain for this example represented in fig.10.

Wavelets analysis is the process of dilations and translations of a mother wavelet, $\psi(x)$ [19]:

$$\{\psi_{j,k}(x) = 2^{j/2}\psi(2^j x - k),\ \ j,k \in Z\} \quad \ldots\ldots\ldots\ldots\ldots(10)$$

where *j* and *k* are the scale and time shift respectively. A function *f(x)* can be represented in terms of the superposition of wavelets of different dilations and translations:

$$f(x) = \sum_{j=-\infty}^{\infty}\sum_{k=-\infty}^{\infty} d_{j,k}\psi_{j,k}(x) \quad \ldots\ldots\ldots\ldots\ldots\ldots\ldots\ldots\ldots\ldots (11)$$

where $\{d_{j,k} : j,k \in Z\}$ are the detailed coefficients of wavelets decomposition. If *f(x)* contains a constant term, then the last equation is modified to include a *scaling function* (*father wavelet), ϕ(x)*:

$$f(x) = c_{00}\phi(x) + \sum_{j=1}^{\infty}\sum_{k=-\infty}^{\infty} d_{j,k}\psi_{j,k}(x) \quad \ldots\ldots\ldots\ldots\ldots\ldots\ldots (12)$$

The mother and father wavelet functions are defined as:

$$\phi(x) = \sum_k h(k)\sqrt{2}\phi(2x - k) \quad \ldots\ldots\ldots\ldots\ldots\ldots\ldots\ldots\ldots (13)$$

$$\psi(x) = \sum_k g(k)\sqrt{2}\phi(2x - k) \quad \ldots\ldots\ldots\ldots\ldots\ldots\ldots\ldots\ldots (14)$$

where the sequences $\{h(k), k \in Z\}$ and $\{g(k), k \in Z\}$ are coefficients of a low pass filter *H(ω)* and a high pass filter *G(ω)*, respectively. They form *a pair of quadrature mirror filters,* which are used in the wavelet decomposition [19]. Applying wavelet transform on signals does not reduce the amount of data for compression or classification. However, elimination of some wavelet coefficients can take place without sacrificing the performance of signal classification.

At each resolution level the wavelet coefficients vary in magnitude and hence their importance to the quality of classification or even compression is different. So in a relative sense some of these coefficients can be eliminated. Making such reduction in the feature extraction coefficients vector would provide a way to reduce the number of free parameters of the classifier, which would lead to a better generalization capability.

For feature extraction experimental EEG signals from different electrodes and for different patients were analyzed and cut into 2.5s sections. Then for the above mentioned H, two plots were made for each section. Those

transformed signals were submitted to wavelet transform instead of the original EEG signals. Wavelet technique was similar to one previously described in [22], so we just summarize the results. The decomposition was fulfilled up to level 5 using Daubechies 8 functions. Analyzing various wavelet coefficients we came to a decision [22] to calculate for each level the mean values of LPF approximation coefficients h(k) . It gave 5 characteristic features for every section. Other variants turned to be less informative.

Figures 9a and 9b show the mean values of wavelet coefficients at different levels for various artifacts. One can compare the plots for regular activities (solid line) with similar plots for various artifacts. Dash-dot lines with circles close to regular activity plots correspond to closed eyes situation when no explicit artifacts were present. It is interesting to mention that Fig.9a and Fig.9b depict different cases of the closed eyes activity (from Fig.7 and Fig.8 correspondingly). As we can see from the figures wavelet coefficients at resolution level r=5 have similar values for different artifacts and for regular activity while they become strongly different as r decreases. This indicates the importance of coefficients at low r for classification purposes. But at the same time the figure illustrates the difficulties of classification as the difference between regular activity (solid line) and various artifacts is small and has different sign for different levels and different artifacts. Despite of the strong difference in the signal amplitudes at Fig. 7 and Fig.8, mean values of wavelet coefficients are practically the same for the two cases. It illustrates the fact that fractal dimension strongly depends on statistical properties but not on the signal amplitude. The most important feature of Fig.9a and Fig.9b is the different character of the regular activity curves and those of artifacts . This feature helps to increase the probability of artifacts selection and classification.

4. Classification of artifacts

Artificial Neural Networks (ANN) was chosen as a classifier [24]. Using this method we again followed the procedure which we described in details in [22] so we briefly repeat its main features. Its main advantage over other classifiers is the ability to learn by training. Furthermore, its complexity (i.e. number of free parameters in the classifier) does not grow with the dimension of the input or the size of the training set [23]. Although there are various types and structures of neural

networks found in the literature, Multilayer Feed forward Networks with the back propagation training algorithm are the most successful and popular [24].

The backpropogation training algorithm is commonly used to iteratively minimize the following cost function with respect to the interconnection weights and neurons thresholds:

$$E = \frac{1}{2}\sum_{1}^{P}\sum_{i=1}^{N}(d_i - z_i)^2 \qquad \text{……..……(15)}$$

Where P is the number of training patterns and N is the number of output nodes. d_i and z_i are the desired and actual responses for output node ***i*** respectively.

The update of the network weights is calculated as:

$$w_{ji}(t+1) = \alpha w_{ji}(t) + \eta x_i f'\left(net_j^k\right)\sum_{l=1}^{N}(d_l - z_l) f'(net_l^0) w_{lj} \text{ …..(16)}$$

Where α is a momentum constant, η is the learning rate, x_i is the input pattern at the iterative sample t, net_N^0 is the input to node N at the output layer and net_j^k is the input to a node j in the *kth* layer.

The training process is terminated either when the Mean-Square Error (MSE) between the observed data and the ANN outcomes for all elements in the training set has reached a pre-specified threshold or after the completion of a pre-specified number of learning epochs.

The neural network was trained to give desired output values of 0.1 and 0.9 to represent 0 and 1. This was done to decrease the training time. Classification performance was further enhanced by interpreting the output in excess of 0.8 as 0.9 and less than 0.2 as 0.1. The Neurosolution software [24] was used for constructing, training and testing the neural network.

5.Experimental results

The experiment was done at the King Hussein Medical Center, Jordan. For the experiment EEG records of 15 healthy volunteers were taken. The electrodes were placed according to the above mentioned 10 – 20 international system and the patients were sitting in the electrically shielded room.

For classification we chose two main types of artifacts – eyes movement and muscle movement- together with the regular activity signals for positions with open eyes and with closed eyes.

Signals from every electrode were cut into small sections 2.5 s long. Visual inspection of strong artifacts was done. Then signals from all electrodes for the same patient at the time when strong artifact was detected were considered as artifacts. Then the dynamics of fractal dimension was plotted for every sample. The samples after processing were submitted to wavelet packet decomposition up to level 5. Wavelet function was Daubechies 8. . For each type of artifacts the wavelet coefficients were averaged over the group of samples and after that the mean wavelet coefficients at levels from 1 to 5 formed 5 features used for training of the neural network classifier. 80% of samples were used for training, then full EEG records including 100% of samples were used for recognition.

Classification results are shown in the Table 2

Table 2

No	Character of the signal	Full identification (%)	Identification as an artifact (%)	Identification as a non-artifact (%)
1	Regular activity (eyes open)	92	0	100
2	Regular activity eyes closed	80	6	94
3 4	Eyes movement Muscle movement	85 78	97 90	3 10

6. Legends of figures

Fig. 1. the internationally standardized *10-20 system* that usually employed to record the spontaneous EEG. In this system 21 electrodes are located on the surface of the scalp, as
shown in Figure 1A, 1B and Figure 1C.

Fig 2.a. The section of a regular EEG signal from a frontal F4 electrode.

Fig. 2b. The H parameter of the regular EEG signal from a frontal F4 electrode as a function of T0.

Fig. 3A. The EEG signal from frontal electrodes together with artifact caused by eyes movement. As we can see the signal represented by strong amplitude.

Fig 3B represented the function of T0 for an artifact caused by eyes movement and taken from the same (as in fig 3A) F4 electrode.

Fig 4a. the signal from the right temporal electrode T4. It is original signal together with artifact caused by eyes movement.

Fig 4.B the results of signal processing of the. in the function H (To). Source signal is same that shown in fig 4a.

Fig.5. Strong artifact signal from T4 electrode caused by a muscle movement. It is shown, that the signal amplitude is greatly increased to compare with the signal together with artifact caused by eyes movement. The frequency of muscle movement artifact as minimum four times greater to compare with eyes movement artifact.

Fig 6. Original signal, detected by electrode P4 at the right parietal part together with muscle movement artifact.

Fig 7. The strong signal from P4 electrode at the right parietal part together with muscle movement artifact.

Fig 8. The regular EEG signals taken at the time when the patient was sitting with his eyes closed. This signal was detected from T4 electrode. As we can see original EEG signal can be represented in different amplitudes, the same muscle movement gives a weak artifact signal

Fig. 9.a The mean values of wavelet coefficients at different levels for various artifacts of high amplitude original signal, that shown in fig 7.. It is shown the plots for regular activities (solid line) with similar plots for various artifacts. Dash-dot lines with circles close to regular activity plots correspond to closed eyes situation when no explicit artifacts were present.

Fig 9.b The mean values of wavelet coefficients of original low-amplitude signal that was represented in fig 8. Its depict different cases of the closed eyes activity for the regular EEG signals taken at the time when the patient was sitting with his eyes closed. As we can see, the form of curves in fig 9b practically the same with curves represented in figure 9.a. Comparing fig 9a and 9b we can come to a conclusion that strong difference in the signal amplitudes at Fig. 7 and Fig.8, mean values of wavelet coefficients are practically the same for the two cases. It illustrates the fact that fractal dimension strongly depends on signal statistical properties but not on the signal amplitude. The most important feature of Fig.9a and Fig.9b is the different character of the regular activity curves and those of artifacts .

Fig 10. Representation of discreet wavelet transform with using filters bank. At each level in the above diagram the signal is decomposed into low and high frequencies. Due to the decomposition process the input signal must be a multiple of 2n where n is the number of levels.

Fig 11. The result of filter bank implementation. This figure illustrated decomposition of signal with 16 samples, frequency range 0 to fn and 3 levels of decomposition.

7. Conclusion

An attempt of automatic detection of EEG artifacts was made using fractal dimension dynamics graphs, wavelet transform and artificial neural networks. Compared with the direct application of wavelet transform to the original EEG signals, this method previously transforms the signal into a plot of its fractal dimension as a function of time. It helps to identify artifact signals with small amplitude through the analysis of their statistical properties.

Total number of analyzed signals was about 300, and the number of artifacts with different amplitudes was more than one thousand, but they were only partially independent

Signals from different electrodes at the same time showed the same artifact. It was good for visual detection of the artifacts used for system training but it increased the number of wrong automatic identifications as at some electrodes the artifact signal was so weak, that the method failed to recognize it. On the other hand a very small artifact signal can be ignored as it does not change strongly the regular signal. We could not fix the exact threshold for artifact detection but visual inspection showed that

artifacts were successfully detected if their amplitude was approximately equal to the amplitude of the regular signal before the moment when the artifact signal appeared.

Conducted researches have shown efficiency of proposed approach to automatic artifact classification, and also confirmed adequacy of proposed features description based on wavelet-transform. However, for more consistent conclusions it is necessary to consider wavelet filters selection problem more thoroughly.

References

1. Handbook of Electroencephalography and Clinical Neurophysiology.- V. 2:
Clinical applications of computer analysis of EEG and other neurophysiological
signals. / Ed. by F.Lopes da Silva et al. - Amsterdam etc., 1986. - 508 p.
2. E. Niedermeyer, F. Lopes da Silva, editors. Electroencephalography: basic
principles, clinical applications, and related fields. Baltimore , 1993. - 1164 p
3. J. Hughes. EEG in clinical practice. Butterworth-Heinemann, 1994
4. O. Rosso **.** 'Wavelet Entropy: A new tool for analysis of short duration Brain
Electrical signals', J. of Neuroscience Methods, 105, pp. 65-75,2001.
5. O. Bai, M. Nakamura, A. Ikeda and H. Shibasaki, "Nonlinear Markov process
amplitude EEG model for nonlinear coupling interaction of spontaneous
EEG," IEEE Transactions on Biomedical Engineering, v. 47, 9 , pp.141-146, 2000.
6 H. Al-Nashash, Y. Al-Assaf, J. Paul, N. Thakor, "Adaptive Modeling of EEG
signals using Markov Process Amplitude," 4th International Workshop On
Biosignal Interpretation, pp. 331-334, June, 2002, Italy.
7. M. Van de Velde , G. Van Erp , P.Cluitmans . Detection of muscle artifact in
the normal human awake EEG. Electroencephalogr Clin Neurophysiol 1998; 107(2)
pp.149-158
8. Vasserman E.L. Geppener V.V., Chernichenko D.A. Methods of allocation
of artifacts in eeg-signals on the basis of dynamic models. BEMI'97,
International Workshop Biomedical Engineering & Medical Informatics.
Gliwice, Poland , 1997.p p.165-167.
9. M. Van de Velde , I. Ghosh , P. Cluitmans .Context related artifact detection

in prolonged EEG recordings. Comput Methods Programs Biomed 1999; 60(3),pp.183-196
10. He Sheng Liu, Tong Zhang, Fu Sheng Yang. A multistage, multimethod
approach for automatic detection and classification of epileptiform EEG. IEEE
Transactions on Biomedical Engineering, v.49 ,12, 2002, pp.1557-1566.
11. M. Shen, L. Sun, F.H.Y. Chan. Method for extracting time-varying rhythms
of encephalography via wavelet packet analysis. IEE Proceedings - Science,
Measurement and Technology, v.148,1,2001,pp. 23-27.
12. J. Britton, B. Jervis, R. Grunewald. Extracting single trial event related
potentials. IEE Proceedings - Science, Measurement and Technology,
v.147,6,2000, pp.382-388
13. U. Hoppe, S. Weiss, R. Stewart, U. Eysholdt. An automatic sequential
recognition method for cortical auditory evoked potentials. . IEEE Transactions
on Biomedical Engineering, v.48 ,2, 2001, pp.154-164.
14. B. West, M. Latka, M. Glaubic-Latka, “Multifractality of cerebral blood
flow,” Physica A 318 (3-4): 2003, pp. 453-460.
15.B. Mandelbrot . J. Van Ness. Fractional Brownian motions, fractional noises
and applications, SIAM Review, 1968, 10, p.422
16. R. M. Cronover. Introduction to fractals and chaos, John and Bartlett
Publishers, N.Y., 2000.
17. B.B. Mandelbrot, The Fractal Geometry of Nature, Freeman, New York,1983
18. D. B. Percival and A. T. Walden, Wavelet Methods for Time Series
Analysis, Cambridge University Press, Cambridge 2000.
19 I. Daubechies. Ten lectures on wavelets, SIAM, Philadelphia, 1992.
20. Afifi A., Azen S. Statistical Analysis . A computer Oriented Approach.
Academic Press, 1979. 488 p.

21.E. Majani, "Biorthogonal wavelets for image compression", Proc. Of the
SPIE, VCIP'94, 1994.
22. H. Al-Nashash, Y. Al-Assaf, B. Lvov, W. Mansour. Classification of material types using laser speckle, wavelets and artifitial neural networks. Materials Evaluation (American Society for Nondestructive Testing) v.59,
No9,2001, pp.1072-1078.
23. S. Mallat and S. Zhong, “Characterization of signals from multiscale edges”,
IEEE Trans. Pattern Anal. Machine Intell., Vol. 14, pp. 710-732, 1992
24. Neurosolution software, “Neural Network software” by NeuroDimension,
Inc, http://www.nd.com, 1999.
25. Jasper HH (1958): Report of the Committee on Methods of Clinical Examination in Electroencephalography. *Electroenceph. Clin. Neurophysiol.* 10: 370-1.
26. Sharbrough F, Chatrian G-E, Lesser RP, Lüders H, Nuwer M, Picton TW (1991): American Electroencephalographic Society Guidelines for Standard Electrode Position Nomenclature. *J. Clin. Neurophysiol* 8: 200-2.
27. Blumhardt LD, Barrett G, Halliday AM, Kriss A (1977): The asymmetrical visual evoked potential to pattern reversal in one half field and its significance for the analysis of visual field effects. *Br. J. Ophthalmol.* 61: 454-61
28. B.V. Lvov, Riad Al-Kasasbeh. 2005.Classification of EEG signals with artifacts, based on fractal dimension analysis, wavelet transform and neural network, Dirasat Journal, v.32. p. 78-90.

Fig.1 A,B,C
Electrode schema position

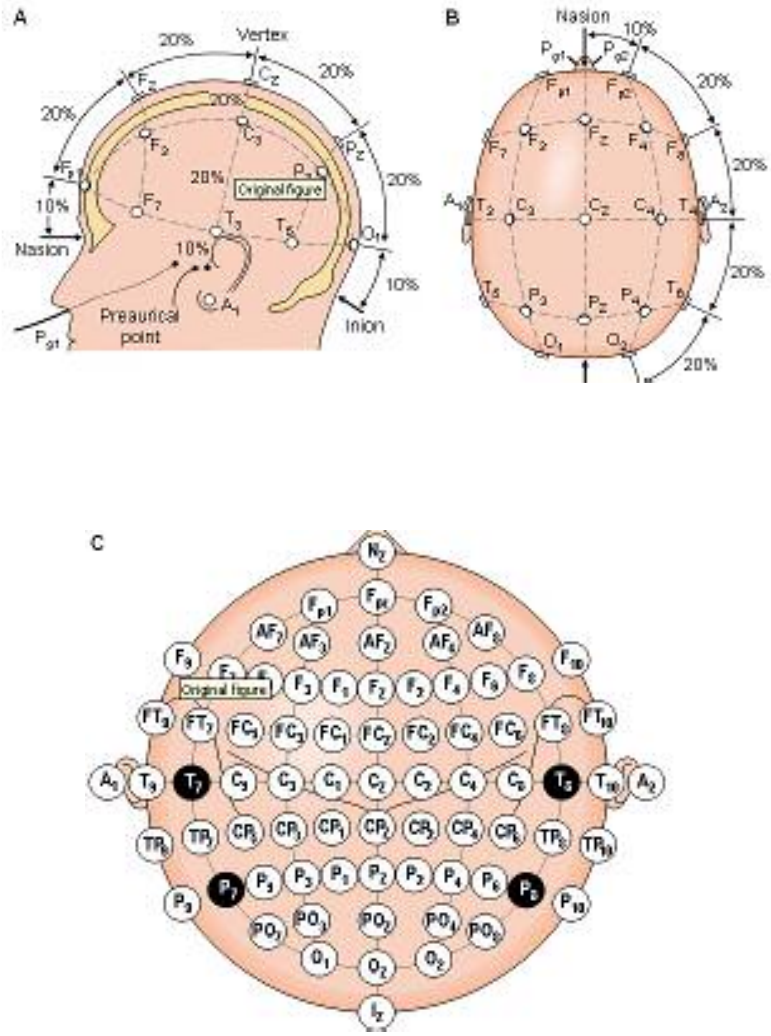

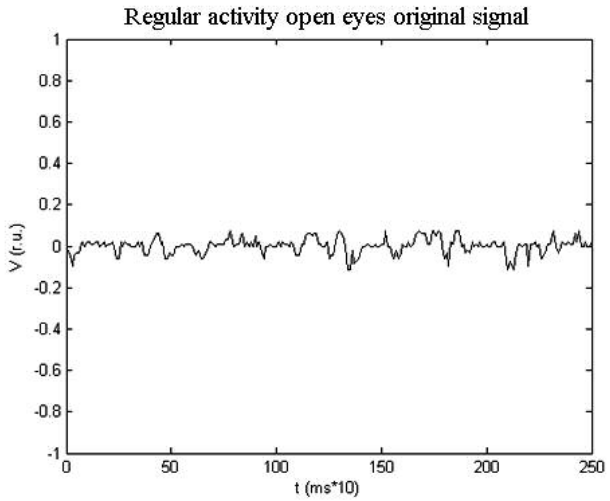
Regular activity open eyes original signal
V (r.u.)
t (ms*10)

Fig.2a

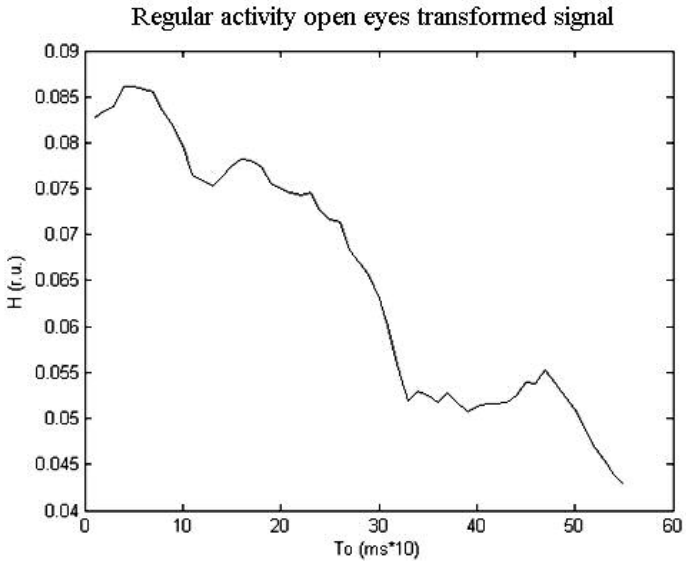
Regular activity open eyes transformed signal
H (r.u.)
To (ms*10)

Fig.2b

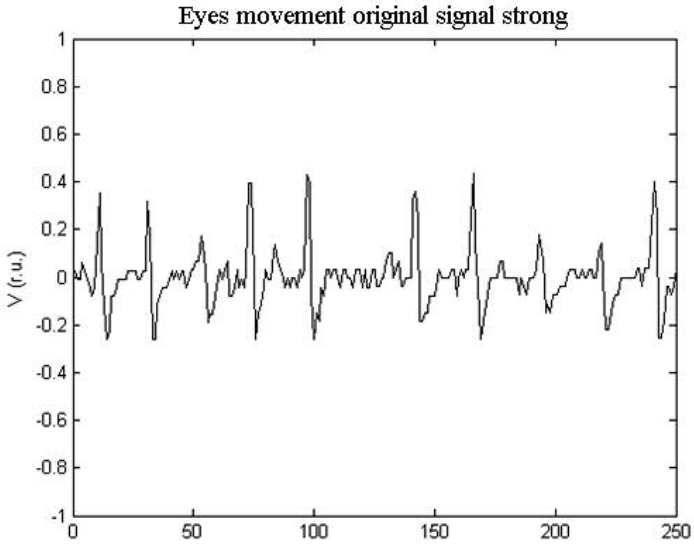
Eyes movement original signal strong
V (r.u.)
1
0.8
0.6
0.4
0.2
0
-0.2
-0.4
-0.6
-0.8
-1
0
50
100
150
200
250

Fig.3a

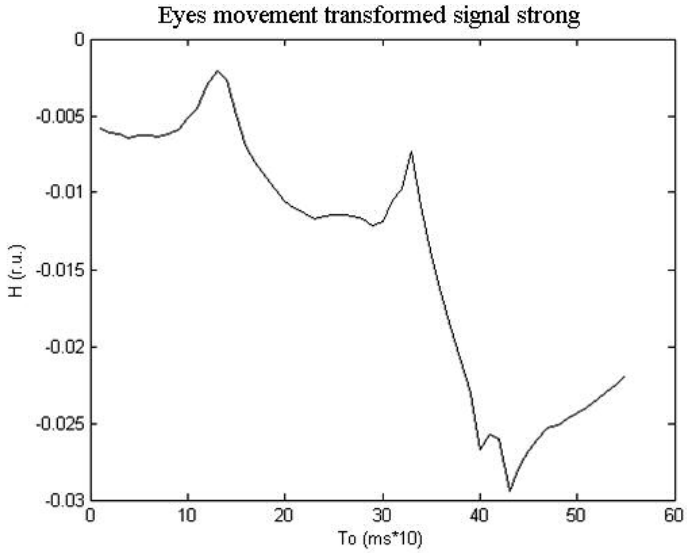
Eyes movement transformed signal strong
H (r.u.)
0
-0.005
-0.01
-0.015
-0.02
-0.025
-0.03
0
10
20
30
40
50
60
To (ms*10)

Fig.3b

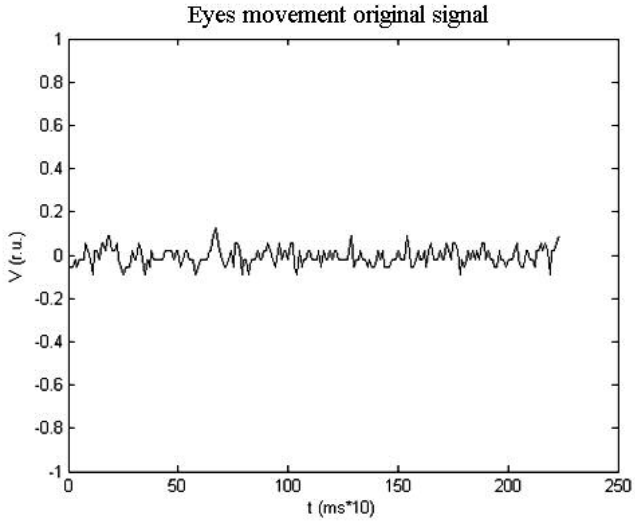
Eyes movement original signal
V (r.u.)
t (ms*10)

Fig.4a

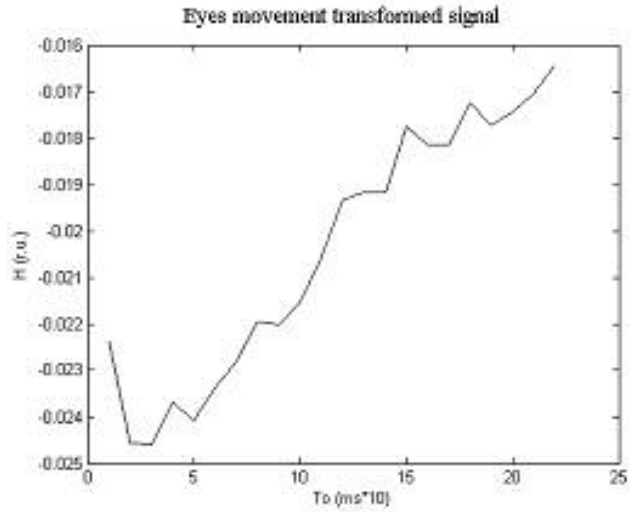
Eyes movement transformed signal
H (r.u.)
To (ms*10)

Fig.4b

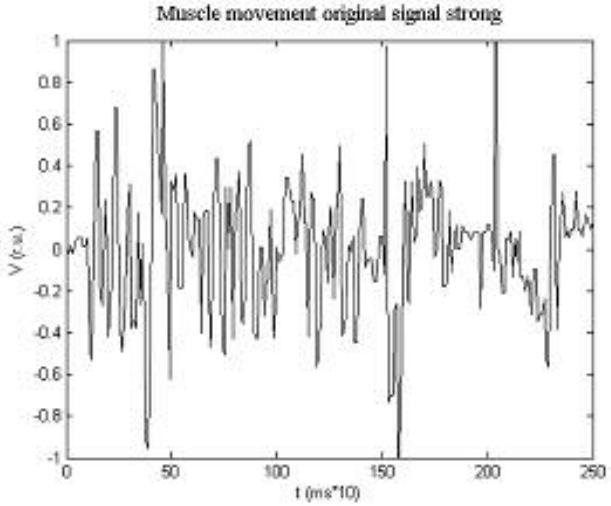
Muscle movement original signal strong
V (r.u.)
t (ms*10)

Fig.5

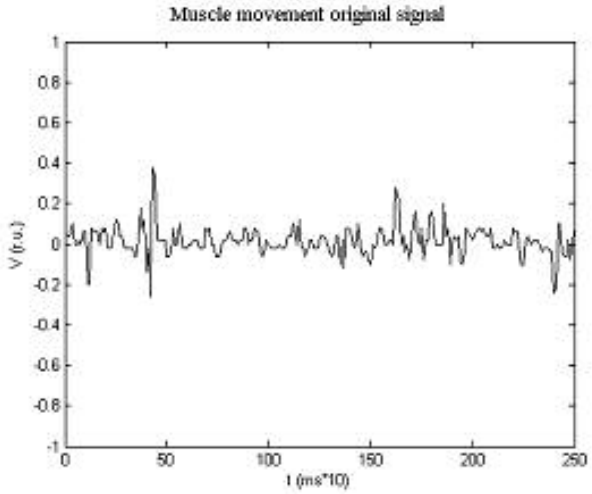
Muscle movement original signal
V (r.u.)
t (ms*10)

Fig.6Fig.7

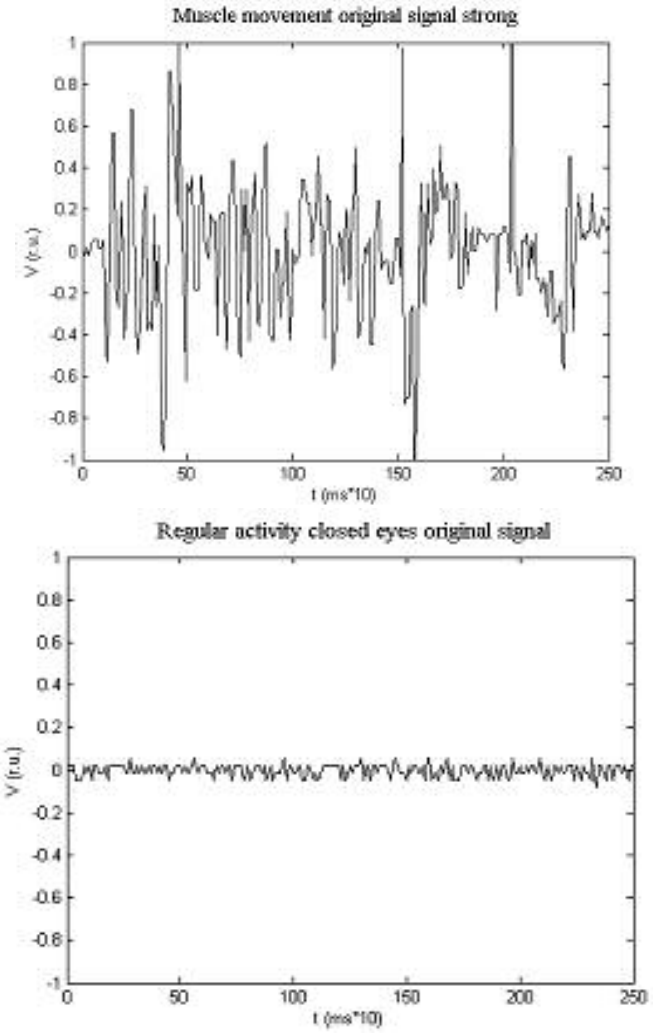
Muscle movement original signal strong
V (r.u.)
t (ms*10)
Regular activity closed eyes original signal
V (r.u.)
t (ms*10)

Fig.8

The mean values of wavelet coefficients of original signal strong

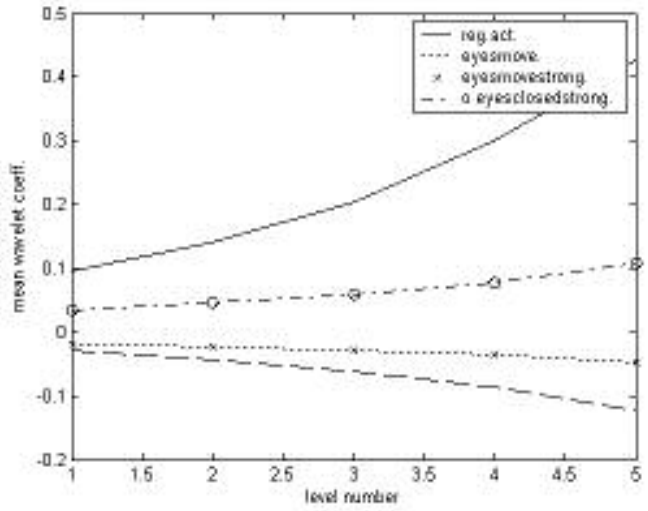

Fig.9a wavelet coefficients at different levels for various artifacts

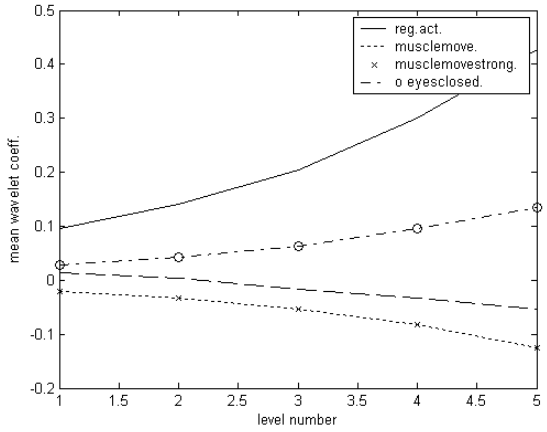

Fig.9b wavelet coefficients at different levels for various artifacts

Fig 10. Block diagram of filter analysis

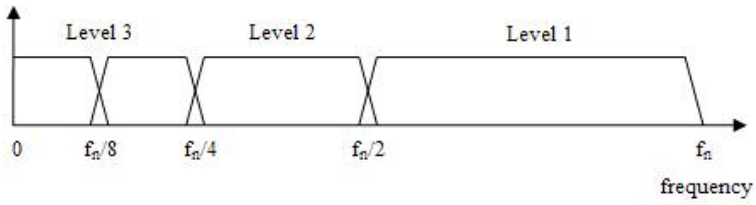

11. Frequency domain representation of the DWT

Received, 10 March, 2005.